NATIONAL ADVISORY COMMITTEE FOR AERONAUTICS

TECHNICAL NOTE 2624

FLAME SPEEDS OF METHANE-AIR, PROPANE-AIR, AND ETHYLENE-AIR MIXTURES AT LOW INITIAL TEMPERATURES

By Gordon L. Dugger and Sheldon Heimel

Lewis Flight Propulsion Laboratory
Cleveland, Ohio

Washington
February 1952

NATIONAL ADVISORY COMMITTEE FOR AERONAUTICS

TECHNICAL NOTE 2624

FLAME SPEEDS OF METHANE-AIR, PROPANE-AIR, AND ETHYLENE-AIR MIXTURES AT LOW INITIAL TEMPERATURES

By Gordon L. Dugger and Sheldon Heimel

SUMMARY

Flame speeds were determined for methane-air, propane-air, and ethylene-air mixtures at -73° C and for methane-air mixtures at -132° C. The data extend the curves of maximum flame speed against initial mixture temperature previously established for the range from room temperature to 344° C. Empirical equations for maximum flame speed u (cm/sec) as a function of initial mixture temperature T_0 were determined to be as follows:

For methane, for T_0 from 141° to 615° K,

$$u = 8 + 0.000160\ T_0^{2.11}$$

For propane, for T_0 from 200° to 616° K,

$$u = 10 + 0.000342\ T_0^{2.00}$$

For ethylene, for T_0 from 200° to 617° K,

$$u = 10 + 0.00259\ T_0^{1.74}$$

Relative flame speeds at low initial temperatures were predicted within approximately 20 percent by either the thermal theory as presented by Semenov or by the diffusion theory of Tanford and Pease. The same order was found previously for high initial temperatures. The low-temperature data were also found to extend the linear correlations between maximum flame speed and calculated equilibrium active-radical concentrations, which were established by the previously reported high-temperature data.

INTRODUCTION

Flame speed is an important combustion property of a fuel-air mixture; as such, it is of interest in both fundamental and applied studies of flame propagation. Data on the effect of initial mixture temperature on flame speed are needed (1) to test the predictions of various theories of flame propagation as to the effect of initial temperature on flame speed in order to obtain a better insight into the process of flame propagation and (2) to add to the literature fundamental data, which should be of value for correlating aircraft-combustor performance with one of the important physical variables, the inlet temperature.

For these reasons, an investigation of the effect of initial temperature on flame speed was undertaken at the NACA Lewis laboratory. Data for methane-air, propane-air, and ethylene-air flames over the temperature range from room temperature to 344° C are presented in reference 1. For these three fuels it is reported that:

(1) Flame speed increased with initial temperature at an increasing rate.

(2) Changes of flame speed, relative to flame speed at room temperature, with change in initial temperature followed the decreasing order: methane, propane, and ethylene.

(3) Relative values of flame speed could be predicted within approximately 20 percent by either a thermal theory or a diffusion theory of flame propagation.

(4) Linear correlations existed between maximum flame speed and calculated equilibrium active-radical concentrations.

In order to test the validity of these results further, and particularly to determine whether any discontinuity would occur in either the flame-speed - temperature curves or the flame-speed - radical-concentration correlations at low temperatures, flame-speed data at low initial temperatures are needed. Low-temperature data are also desirable in order to extend the range of temperatures covered to the low temperatures which might be encountered in flight.

Flame-speed data for initial temperatures of -73° and -132° C for methane-air mixtures and -73° C for propane-air and ethylene-air mixtures are included herein. The flame speeds were computed from measurements based on the outer edge of the shadow cast by the laminar Bunsen cone of a flame seated on a nozzle. A velocity profile of one of the nozzles is also presented and discussed with regard to the method used in calculating flame speed.

SYMBOLS

The following symbols are used in this report:

A	longitudinal cross-sectional area of cone, measured by a planimeter (sq cm)
b, c	constant for a given fuel
$D_{i,r}$	relative diffusion coefficient of given active radical with respect to other radicals
E	activation energy (cal/gram-mole)
h	height of cone (cm)
l	slant height or length of generating curve (cm)
n	constant exponent for given fuel
p_i	mole fraction or partial pressure of i^{th} radical in burned gas
p_H	partial pressure of hydrogen atom in burned gas
p_O	partial pressure of oxygen atom in burned gas
p_{OH}	partial pressure of hydroxyl radical in burned gas
R	gas constant (cal/(gram-mole) (^oK))
S	lateral surface area (sq cm)
T_f	flame temperature (^oK)
T_0	initial mixture temperature (^oK)
u	flame speed (cm/sec)

EXPERIMENTAL PROCEDURE

Fuels. - The minimum purities stated by the suppliers of the methane and the ethylene were 99.0 and 99.5 percent, respectively. The propane had a minimum purity of 95.0 percent, the major impurities being ethane and isobutane.

Apparatus. - The apparatus, with the exception of the conventional parallel-beam shadowgraph system, is diagrammatically illustrated in figure 1. The apparatus and the experimental technique were the same as reported in reference 1, except that provision was made for drying the air with activated alumina and for precooling the fuel-air mixture. A nozzle-type burner was chosen in order to obtain laminar flow in a short over-all burner length so that the whole burner assembly could be cooled by submerging it in an 18-centimeter-diameter by 33-centimeter-deep Dewar vessel. Details of construction of the burner are shown in figure 2. The burner proper was made of brass and had an over-all length of 30.5 centimeters.

The fuel and the dry air were mixed and fed through the inlet tube T to the manifold V, from which it entered the burner by means of 16 small holes U equally spaced circumferentially about the base. It then passed through the straight section S and through four calming screens O, which were supported by brass rings R and sealed by neoprene O-rings Q. The mixture was then accelerated by a Mache-Hebra type brass nozzle N (reference 2) and further accelerated by a small ceramic nozzle H, which was cemented to the brass nozzle.

The ceramic nozzle was added to the original brass nozzle after it was found that such an arrangement aided in stabilizing the flame. The improved stability was presumably due to the reduced thermal gradient between flame and nozzle since stable, regularly shaped flames were obtained only after the flame had been allowed to heat the ceramic nozzle to a temperature 60° to 100° C higher than the gas temperature. Tests made with a propane-air mixture at room temperature indicated that this difference between the temperature of the short ceramic nozzle and the gas temperature did not appreciably affect flame speed. For methane and propane, the ceramic nozzle had a throat diameter of 12.7 millimeters; for ethylene, 6.4 millimeters. These nozzles were turned from round stock by cutting an axial hole to the desired throat diameter and then rounding the upstream edge of the hole to approximately a 1.6-millimeter radius. The nozzle disks were 3.2 millimeters thick.

For the data obtained at -73° C, the burner as described was submerged in a bath of dry ice in acetone and was supported on the lip of the Dewar vessel (L, fig. 1) by the steel flange I, which was screwed onto the brass nozzle. For the data at -132° C, for which liquid nitrogen was used as the coolant, it was found necessary to jacket the lower three-quarters of the burner with air to prevent overcooling and consequent

condensation of oxygen from the primary air. This was accomplished by bolting a steel can (K, fig. 1) to a flange soldered to the brass nozzle. The desired nozzle-outlet temperature was then obtained by varying the level of liquid nitrogen with respect to the top of the air jacket.

The gas temperature was measured between runs by a bare 28-gage copper-constantan thermocouple, which had a soft-solder head of approximately 1.5-millimeters diameter at the junction. It was supported in a piece of pyrex tubing with a right-angle bend such that the thermocouple leads extended downward (along the axis of the gas stream) for a distance of 6 centimeters. The wall temperature of the ceramic nozzle was measured by another copper-constantan thermocouple. For the -73° C data, it was believed that errors in the gas-temperature readings due to radiation and lead-conduction losses were of the order of ±1 percent. For the -132° C data, errors due to radiation and lead conduction when the thermocouple was placed in the nozzle throat were greater. A correction was estimated by the following method: Gas-temperature readings were taken with the junction at depths of 0.3 and 5.0 centimeters below the top surface of the ceramic nozzle. Of these two temperature readings, the 5-centimeter reading was subject to smaller lead-conduction and radiation errors because the junction was well inside the cold nozzle. With the two gas-temperature readings and the ceramic-nozzle temperature known for flow without burning, an estimate was made of the correction to be applied to the 5-centimeter reading in order to obtain the correct temperature of the gas leaving the nozzle throat (initial mixture temperature). It was assumed that the lead-conduction error was negligible; the radiation and wall-to-gas heat-transfer corrections (estimated from reference 3) totaled 5° C. The initial mixture temperature was therefore taken to be the 5-centimeter reading plus 5° C.

Determination of flame speed. - Shadowgraphs of the flames were made by a parallel-beam system. Flame speeds were determined from measurements based on the outer edge of the cone shadow by the total-area method, wherein the average normal flame speed is equal to the volume rate of flow of the unburned mixture divided by the surface area of the cone formed by the combustion zone. This surface area was determined by assuming that the flame surface can be approximated by the relation for conical surfaces of revolution

$$S = \pi A \, l/h$$

RESULTS AND DISCUSSION

Velocity profile of nozzle. - In figure 3 a velocity profile is shown for the 12.7-millimeter ceramic nozzle (on the brass nozzle) for an average air-flow velocity (volumetric flow rate divided by nozzle-throat area) of 124 centimeters per second at 25° C. The profile was obtained

by means of a hot-wire-anemometer probe, which was calibrated the same day by traverses of fully developed laminar flow (reference 4) in a 25-millimeter-inside-diameter tube. The calibration curve was established by assuming the local velocity at the axis of the 25-millimeter tube to be twice the average velocity and the average velocity to be equal to the local velocity at a distance from the tube axis equal to 0.707 times the tube radius. This condition was experimentally confirmed within ±5 percent, which is believed to be the accuracy of the measurements.

The average velocity computed from the anemometer readings was 131 centimeters per second, assuming a linear velocity gradient from the outermost data points to the nozzle wall. While the central portion of the velocity profile is fairly flat, the local velocities over this portion are of the order of 20 percent higher than the average air-flow velocity. Since flame-speed values based on a local velocity which was assumed to be equal to the average velocity would thus have been in great error, it was decided to use the total-area method of flame-speed measurement (described in the section Determination of flame speed) for nozzle flames, as was previously done with tube flames (reference 1). While the two-stage nozzle referred to here is an unusual case, it is believed that an appreciable error would result from ignoring the boundary-layer effect for any small-diameter nozzle.

Flame speeds based on outer edge of shadow. - As indicated in references 5 and 6, the maximum density gradient is more nearly represented by the outer edge of the shadow than by the inner edge because of the manner in which the shadow of a flame cone is produced. If the locus of maximum density gradient is taken to correspond to the flame front, absolute values of flame speed should be based on the outer edge of the shadow.

In figure 4, flame speed is plotted as a function of equivalence ratio (fraction of stoichiometric fuel-air ratio) at initial mixture temperatures of -73° C for methane-air, propane-air, and ethylene-air, and at -132° C for methane-air. Stream flows were maintained in the laminar range at the Reynolds numbers indicated in figure 4. Each of the curves shows that the maximum flame speed for a given temperature occurs at an equivalence ratio slightly greater than 1.0 (richer than stoichiometric).

In order to compare the low-temperature flame speeds with the previously reported high-temperature flame speeds, it was necessary to convert the high-temperature values, which were based on the inner edge of the flame-cone shadow, to values based on the outer edge of the shadow. This conversion was accomplished by multiplying the inner-edge values by the following conversion factors (reference 1): for methane, 0.900; for propane, 0.885; and for ethylene, 0.849.

The flame-speed maximums from figure 4, as well as the converted flame-speed maximums from reference 1, are plotted against initial mixture temperature in figure 5 to show that the low-temperature points extend the curves previously established for the range from room temperature to 617° K. No discontinuity occurs at the low temperatures studied. It appears that the curves might be extrapolated to some small value of flame speed at 0° K.

It was found that the effect of initial mixture temperature (T_0, °K) on maximum flame speed (u, cm/sec) could be represented by empirical equations of the type

$$u = b + cT_0^n \tag{1}$$

where b, c, and n are constants for a given fuel. The equations, which were determined by picking an integer for b which gave a straight line on a logarithmic plot of (u-b) against T_0 (fig. 6) and then determining c and n by the method of least squares, are:

For methane, for T_0 from 141° to 615° K,

$$u = 8 + 0.000160\ T_0^{2.11}$$

For propane, for T_0 from 200° to 616° K,

$$u = 10 + 0.000342\ T_0^{2.00}$$

For ethylene, for T_0 from 200° to 617° K,

$$u = 10 + 0.00259\ T_0^{1.74}$$

Comparison of experimental data with relative values predicted by theoretical equations. - It is shown in references 1 and 7 that, for the purpose of predicting the relative effect of temperature on flame speed, the thermal-theory equations of Semenov (reference 8) might be reduced to the following expressions:

For a monomolecular reaction controlling,

$$u \propto \sqrt{T_f^{3.83} T_0^2 \frac{e^{(-E/RT_f)}}{(T_f - T_0)^2}} \tag{2}$$

For a bimolecular reaction controlling,

$$u \propto \sqrt{T_f^{4.9} T_0^2 \frac{e^{(-E/RT_f)}}{(T_f - T_0)^3}} \tag{3}$$

These reduced expressions involve the assumption that the relations between the physical properties and the temperature for the mixture are reasonably near those for air.

The diffusion theory of Tanford and Pease (reference 9) was also considered for the purpose of predicting the relative effect of temperature on flame speed in reference 1. The reduced expression which resulted from their square-root-law equation is:

$$u \propto \sqrt{\left(\sum_i p_i D_{i,r}\right) \frac{T_o^2}{T_f^{1.33}}} \tag{4}$$

where

$$\sum_i p_i D_{i,r} = 6.5\, p_H + p_{OH} + p_O$$

Comparisons of the relative effects of initial temperature on flame speed as predicted by the reduced equations (2), (3), and (4) for methane, propane, and ethylene are presented in figures 7(a), 7(b), and 7(c), respectively. Each of the curves was plotted by computing flame speeds at various temperatures relative to the experimental value of maximum flame speed at 25° C. The experimental results are represented by the dashed curves.

The values used in plotting the curves in figure 7 (and fig. 8, discussed later) are presented in table I. The flame temperatures quoted in table I were based on sodium D-line measurements of flame temperatures of mixtures at 25° C (reference 10). The changes in flame temperature with initial temperature were assumed to be the same as for the theoretical adiabatic flame temperature (reference 11); that is, the difference between computed adiabatic flame temperature and sodium D-line temperature was taken to be constant for a given mixture. The equilibrium radical concentrations were computed by the graphical method of reference 12. Relative flame speeds at low initial temperatures are predicted within approximately 20 percent by either the thermal theory or the square-root law, as was also found to be the case for high initial temperatures (reference 1).

The difference between adiabatic and sodium D-line temperatures increased in going from methane to propane to ethylene. It might be argued that since this difference increased from fuel to fuel in the same order as the sodium D-line flame temperatures increased at the reference initial temperature of 25° C, the difference should not be constant for a given fuel but should increase as the flame temperature increases. In other words, the sodium D-line temperature of 2400° K for ethylene at an initial temperature of 344° C might be too high. On this

premise, the predictions of equations (2), (3), and (4) were recomputed for ethylene for a flame temperature of 2350° K at the initial temperature of 344° C and were found to give predicted flame speed values of 196.6, 214, and 170.6 centimeters per second, respectively. These predicted values are well within 20 percent of the experimental value of 196.0 and compare with the predicted values of 218.2, 236.8, and 189.8 listed in table I.

In general, for elevated temperatures the thermal-theory values were high and the square-root-law values were low; whereas for low temperatures the values predicted by the two theories were substantially the same. However, even qualitative observations regarding the relative merits of the two theories are subject to the assumptions made and the flame temperatures and activation energies used. (See references 1 and 7 for examples and further discussion.)

Correlation of flame speeds with active-radical concentrations. - In reference 1, linear correlations were found between maximum flame speed and calculated equilibrium active-radical concentrations for mixtures of methane-air, propane-air, and ethylene-air at high initial temperatures. Straight-line correlations resulted from using (1) a summation of effective relative concentrations of hydrogen atoms, hydroxyl radicals, and oxygen atoms computed at sodium D-line flame temperatures; (2) hydrogen-atom concentrations alone computed at sodium D-line flame temperatures; (3) hydrogen-atom concentrations alone computed at adiabatic flame temperatures. In figure 8, the maximum flame speeds at low initial temperatures are plotted against active-radical concentrations together with the converted high-temperature data.

The straight lines of figure 8 indicate that, at least for the three fuels studied, the maximum flame speed of a gaseous fuel may be accurately estimated over a considerable range of initial mixture temperature when the experimental values at two temperatures are known and sufficient data exist to compute the adiabatic flame temperatures and, hence, the equilibrium hydrogen-atom concentrations.

The slopes of the correlations in figure 8 are greater than those shown in the correlations between flame speed and radical concentration in reference 13. In considering this difference, it must be remembered that, for a given correlation line in figure 8(a), initial mixture temperature varied while equivalence ratio (composition) and fuel type were fixed; whereas in reference 13 fuel type varied while initial temperature was fixed and equivalence ratios were essentially the same. The data reported herein indicate that flame speeds for a given fuel vary from five- to tenfold over the range of temperatures studied, whereas in reference 13 a range of only twofold was covered in the flame speeds for different fuels at the same initial temperature. However, the flame temperature and the radical-concentration ranges are of the same order in

both studies. The reasons for the difference in slope may, in part, be attributed to the temperature dependency of the other factors, such as reaction rate, in the original Tanford and Pease equation (references 9 and 14). Inasmuch as the present data are self-consistent, it is valid to use these data to predict the effect of initial mixture temperature on maximum flame speed.

SUMMARY OF RESULTS

An investigation of the laminar flame speeds of methane-air, propane-air, and ethylene-air mixtures at low initial temperatures, together with the earlier work at high initial temperatures, gave the following results:

1. In a plot of maximum flame speed against initial mixture temperature, no discontinuity was revealed as lower temperatures were reached. Empirical equations for maximum flame speed u (cm/sec) as a function of initial mixture temperature T_0 were determined as follows:

For methane, for T_0 from 141° to 615° K,

$$u = 8 + 0.000160\ T_0^{2.11}$$

For propane, for T_0 from 200° to 616° K,

$$u = 10 + 0.000342\ T_0^{2.00}$$

For ethylene, for T_0 from 200° to 617° K,

$$u = 10 + 0.00259\ T_0^{1.74}$$

2. Both the thermal-theory equations presented by Semenov and the diffusion theory of Tanford and Pease were used to predict relative flame speeds within approximately 20 percent for the temperatures and gases studied, thus extending the previously established comparison made at high temperatures.

3. The low-temperature data were also found to extend the linear correlations between maximum flame speeds and calculated equilibrium active-radical concentrations, which were previously established by the high-temperature data.

4. A velocity traverse of one of the burner nozzles showed that local velocities in the nearly flat central portion of the velocity profile were of the order of 20 percent higher than the average velocity

over the entire nozzle throat area. This difference indicates the considerable error which might result from basing flame speed on a local velocity assumed equal to the average velocity for a converging nozzle (for example, in the angle method).

Lewis Flight Propulsion Laboratory
National Advisory Committee for Aeronautics
Cleveland, Ohio, October 16, 1951

REFERENCES

1. Dugger, Gordon L.: Effect of Initial Mixture Temperature on Flame Speed of Methane-Air, Propane-Air, and Ethylene-Air Mixtures. NACA TN 2374, 1951.

2. Mache, Heinrich, und Hebra, Alexius: Zur Messung der Verbrennungsgeschwindigkeit explosiver Gasgemische. Akademie der Wissenschaften in Wien. Math.-naturw. Klasse. Sitzungsberichte. Vol. 150, Abt. IIa, 1941, S. 157-174.

3. McAdams, William H.: Heat Transmission. McGraw-Hill Book Co., Inc., 2d ed., 1942, pp. 185, 225.

4. Dodge, Russell A., and Thompson, Milton J.: Fluid Mechanics. McGraw-Hill Book Co., Inc., 1st ed., 1937, pp. 171-175.

5. Linnett, J. W., and Hoare, M. F.: Burning Velocities in Ethylene-Air-Nitrogen Mixtures. Third Symposium on Combustion and Flame and Explosion Phenomena, The Williams & Wilkins Co. (Baltimore), 1949, pp. 195-203; discussion by Kurt Wohl, pp. 203-204.

6. Grove, J. R., Hoare, M. F., and Linnett, J. W.: The Shadow Cast by a Bunsen Flame, Its Production and Usefulness. Trans. Faraday Soc. (London), vol. 46, pt. 9, Sept. 1950, pp. 745-755.

7. Dugger, Gordon L.: Effect of Initial Mixture Temperature on Flame Speeds and Blow-Off Limits of Propane - Air Flames. NACA TN 2170, 1950.

8. Semenov, N. N.: Thermal Theory of Combustion and Explosion. III - Theory of Normal Flame Propagation. NACA TM 1026, 1942.

9. Tanford, Charles, and Pease, Robert N.: Theory of Burning Velocity. II. The Square Root Law for Burning Velocity. Jour. Chem. Phys., vol. 15, no. 12, Dec. 1947, pp. 861-865.

10. Perry, John H.: Chemical Engineers' Handbook. McGraw-Hill Book Co., Inc., 2d ed., 1941, p. 2410.

11. Hottel, H. C., Williams, G. C., and Satterfield, C. N.: Thermodynamic Charts for Combustion Processes, Pt. I. John Wiley & Sons, Inc., 1949.

12. Huff, Vearl N., and Calvert, Clyde S.: Charts for the Computation of Equilibrium Composition of Chemical Reactions in the Carbon-Hydrogen-Oxygen-Nitrogen System at Temperatures from 2000° to 5000° K. NACA TN 1653, 1948.

13. Simon, Dorothy Martin: Flame Propagation. III. Theoretical Consideration of the Burning Velocities of Hydrocarbons. Jour. Am. Chem. Soc., vol. 73, no. 1, Jan. 1951, pp. 422-425.

14. Dugger, Gordon L.: The Effect of Initial Mixture Temperature on Burning Velocity. Jour. Am. Chem. Soc., vol. 73, no. 5, May 1951, p. 2398.

15. Chamberlain, G. H. N., et Walsh, A. D.: L'oxydation lente de l'éther diisopropylique dans l'intervalle de températures 360° - 460° C. Revue de L'Institut Francais du Pétrole et Annales des Combustibles Liquides, Vol. IV, No. 7, Juillet 1949, p. 315.

16. Jost, Wilhelm: Explosion and Combustion Processes in Gases. McGraw-Hill Book Co., Inc., 1946.

TABLE I - PREDICTED RELATIVE FLAME SPEEDS

Fuel	Equivalence ratio (a)	Activation energy according to thermal theory $\left(\frac{\text{kcal}}{\text{g-mole}}\right)$	Initial temperature (°C)	Flame temperature (°K)		Equilibrium radical pressure (total pressure of 1 atm) (d)				Predicted maximum flame speed, relative to max. flame speed at 25° C (cm/sec)			Experimental flame speed (cm/sec)
				Theoretical adiabatic (b)	Based on sodium D-line (c)	P_H (adiabatic)	P_H (sodium D-line)	P_{OH} (sodium D-line)	P_O (sodium D-line)	Thermal unimolecular (e)	Thermal bimolecular (f)	Square-root law (g)	
Methane	1.122 (10.5 volume percent)	51[h]	-132	2053	2008	0.270×10^{-3}	0.203×10^{-3}	0.282×10^{-3}	0.003×10^{-3}	10.5	10.1	11.9	13.4
			-73	2090	2045	.340	.255	.407	.005	17.5	17.1	18.8	19.2
			25	2153	2108[i]	.520	.395	.635	.013	34.0	34.0	34.0	34.0[j]
			34	2159	2114	.538	.408	.665	.014	35.9	36.0	35.5	35.5
			94	2197	2152	.670	.517	.890	.023	50.0	50.9	47.3	48.0
			150	2251	2186	.810	.630	1.13	.038	66.0	68.2	60.0	62.0
			206	2268	2221	.980	.770	1.45	.057	85.6	89.7	74.6	80.0
			261	2298	2253	1.16	.915	1.80	.084	107.7	114.5	90.5	95.0
			344	2345	2300	1.48	1.17	2.44	.141	148.2	160.9	118.3	133.0
Propane	1.049 (4.2 volume percent)	38[k]	-73	2204	2148	0.460×10^{-3}	0.299×10^{-3}	1.17×10^{-3}	0.052×10^{-3}	22 .8	22.2	23.0	23.8
			25	2253	2198	.590	.420	1.62	.086	40.2	40.2	40.2	40.2[j]
			29	2255	2200	.607	.432	1.65	.088	41.3	41.3	41.1	41.5
			93	2288	2233	.700	.525	2.00	.124	55.5	56.4	54.4	56.4
			149	2317	2262	.860	.627	2.38	.169	70.2	72.5	67.8	69.2
			204	2345	2290	1.00	.757	2.80	.228	86.8	91.0	82.6	87.0
			260	2371	2316	1.18	.855	3.26	.300	105.7	112.3	98.7	105.0
			343	2412	2357	1.43	1.07	4.10	.480	139.0	150.8	126.9	141.2
Ethylene	1.165 (7.5 volume percent)	40[l]	-73	2302	2198	1.13×10^{-3}	0.629×10^{-3}	0.94×10^{-3}	0.035×10^{-3}	35.8	35.0	37.5	35.5
			25	2352	2248	1.46	.855	1.28	.061	64.0	64.0	64.0	64.0[j]
			34	2356	2252	1.48	.875	1.32	.064	66.9	67.0	66.8	66.8
			94	2386	2282	1.72	1.02	1.64	.093	88.3	89.8	86.0	86.0
			150	2413	2309	1.98	1.17	1.95	.126	111.3	114.8	106.1	105.7
			206	2440	2336	2.23	1.35	2.33	.171	137.6	144.0	128.0	126.0
			261	2465	2361	2.50	1.53	2.70	.222	166.1	176.1	151.0	153.0
			344	2504	2400	3.00	1.83	3.39	.331	218.2	236.8	189.8	196.0

[a]Fraction of stoichiometric fuel-air ratio at which maximum flame speed occurred.

[b]Computed by method of reference 11.

[c]Computed by subtracting from the adiabatic flame temperature a constant equal to difference between adiabatic and sodium D-line values (reference 10) at 25° C.

[d]Computed by method of reference 12.

[e]Computed from equation (2).

[f]Computed from equation (3).

[g]Computed from equation (4).

[h]Reference 15.

[i]Computed using same difference between adiabatic and sodium D-line values as was found for 10.0 percent methane.

[j]Obtained from fig. 5 by interpolation.

[k]Reference 16, p. 437.

[l]Reference 5.

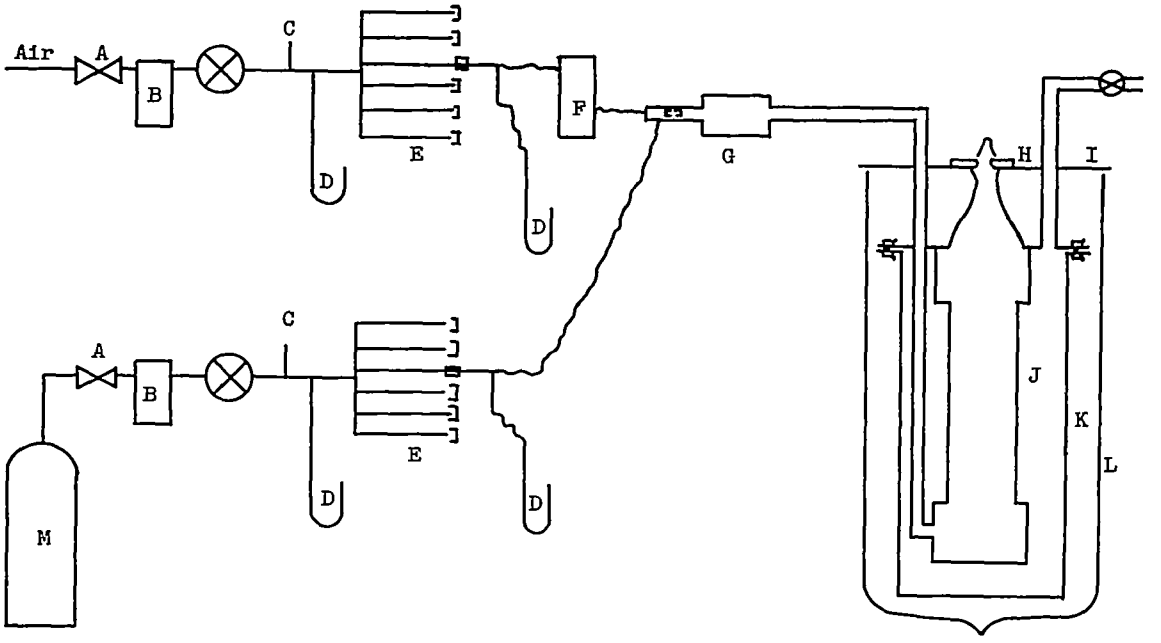

A Pressure regulators
B Filters
C Thermocouples for temperature at orifice
D Manometers
E Critical-flow-orifice manifolds
F Activated-alumina drier
G Mixer
H Ceramic nozzle
I Steel flange
J Burner (see fig. 2 for detail)
K Air jacket
L Dewar vessel
M Fuel cylinder

Figure 1. - Diagrammatic sketch of experimental apparatus.

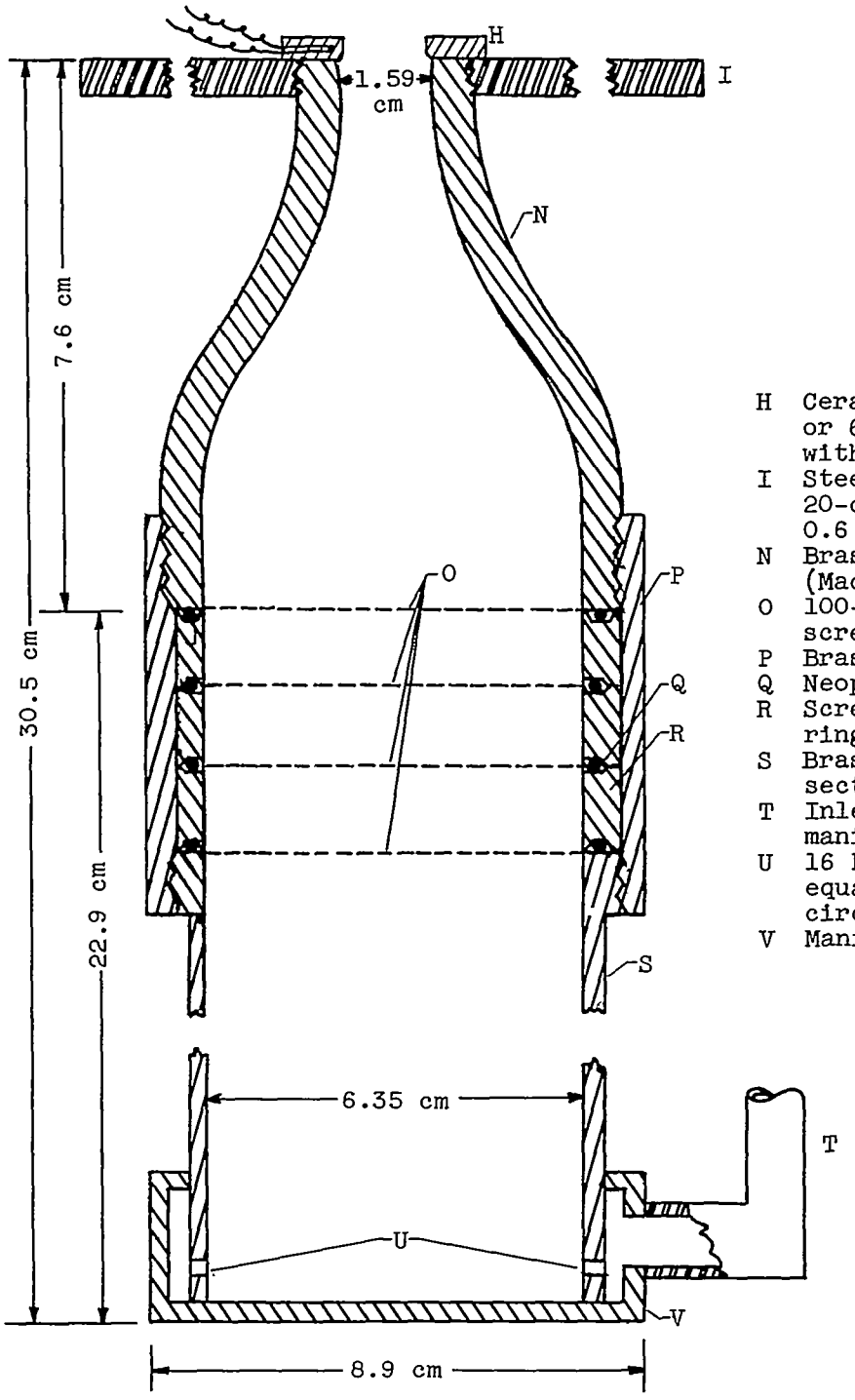

Figure 2. - Detail of low-temperature burner.

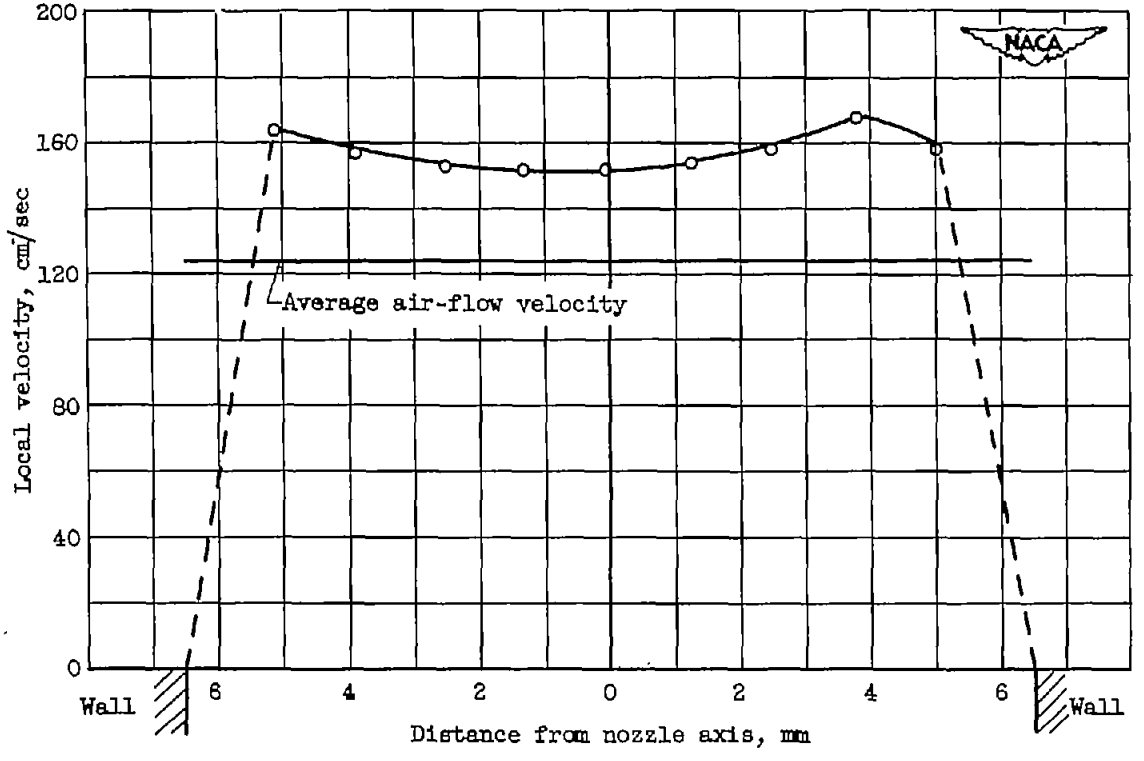

Figure 3. - Velocity profile above a 12.7-millimeter ceramic nozzle cemented to the brass Mache-Hebra nozzle. Air temperature, 25° C; Reynolds number, 1020.

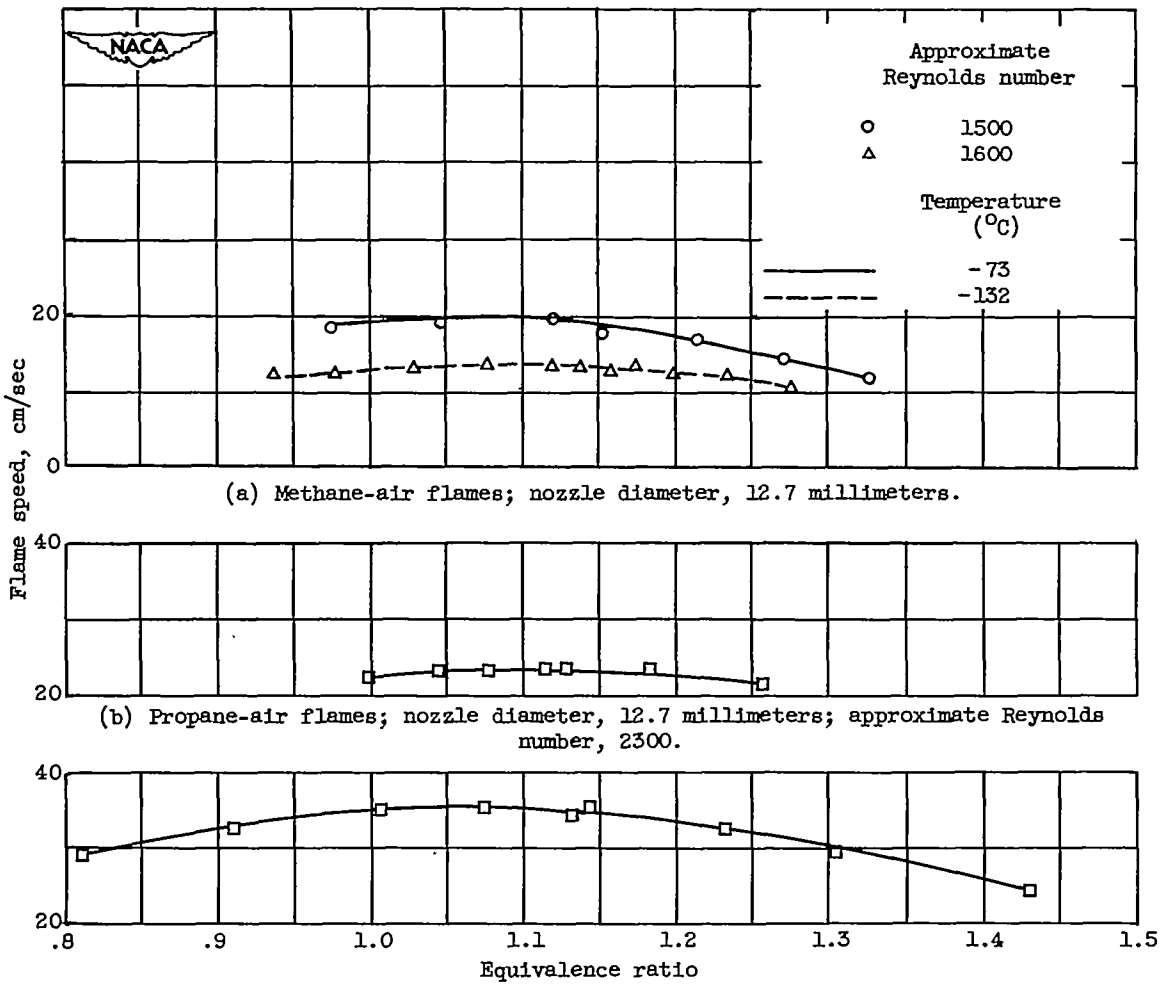

(a) Methane-air flames; nozzle diameter, 12.7 millimeters.

(b) Propane-air flames; nozzle diameter, 12.7 millimeters; approximate Reynolds number, 2300.

(c) Ethylene-air flames; nozzle diameter, 6.4 millimeters; approximate Reynolds number, 1400.

Figure 4. - Flame speed as function of equivalence ratio (fraction of stoichiometric fuel-air ratio) at various temperatures.

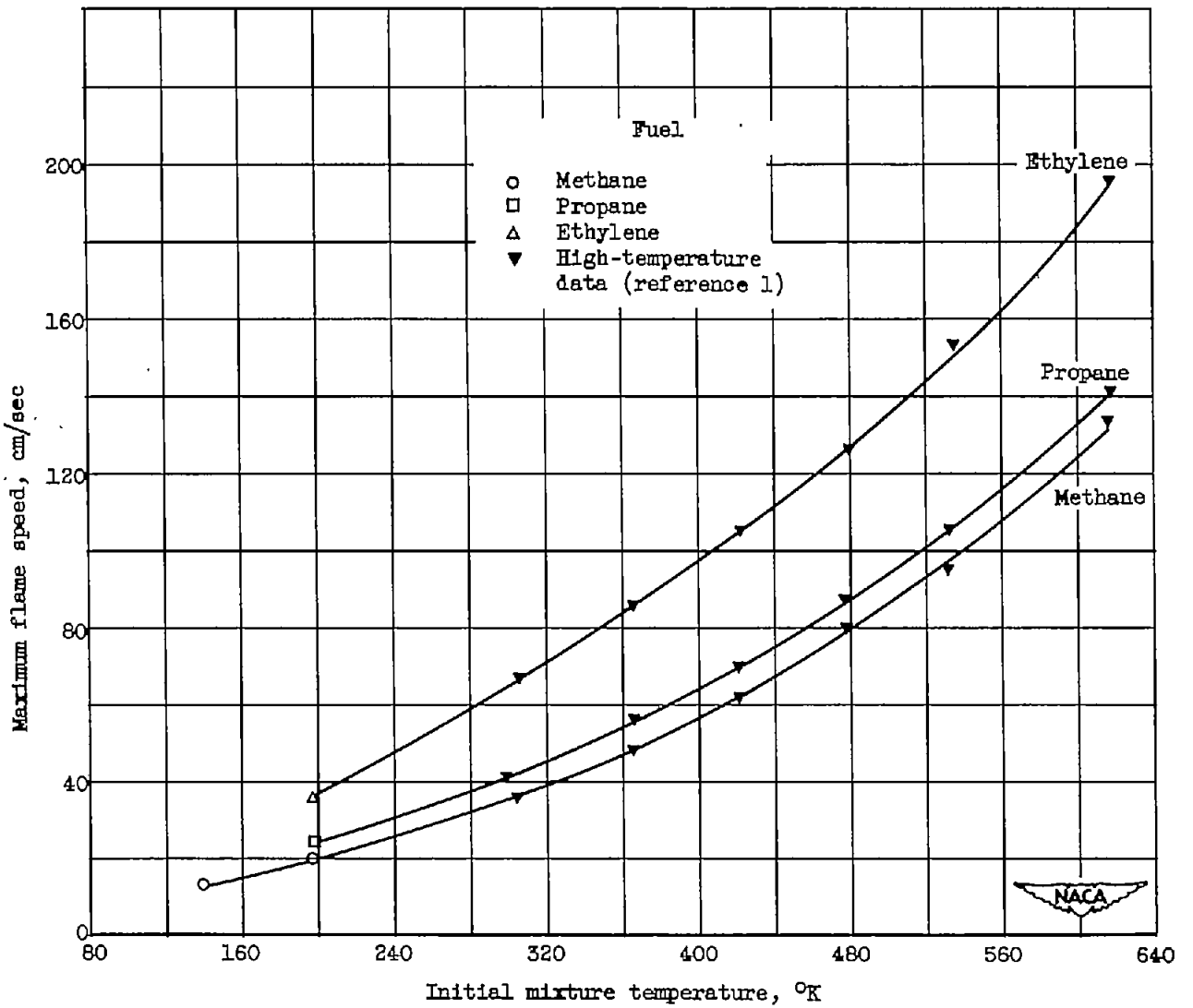

Figure 5. - Effect of initial temperature on maximum flame speed.

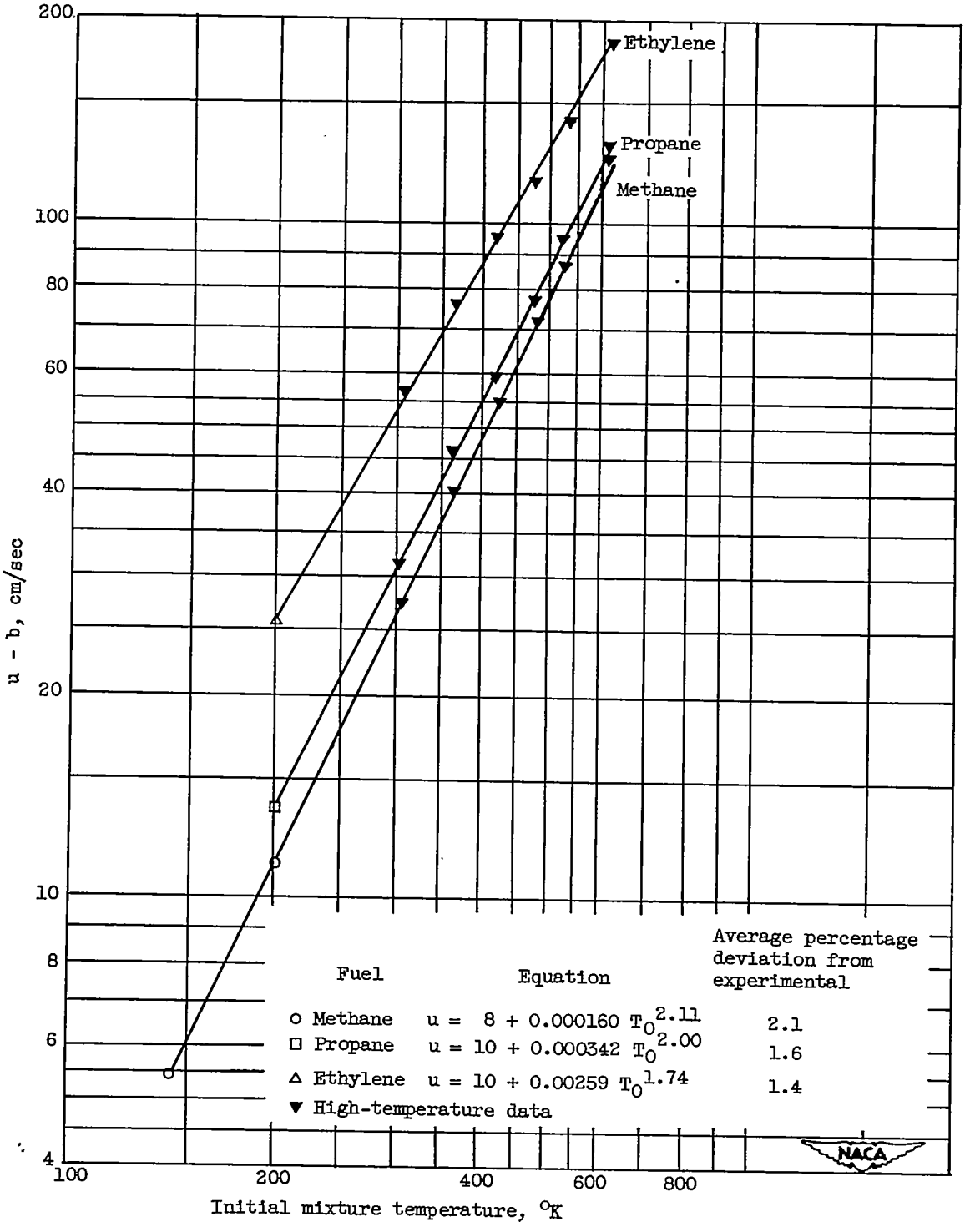

Figure 6. - Empirical equations for maximum flame speed as function of initial mixture temperature.

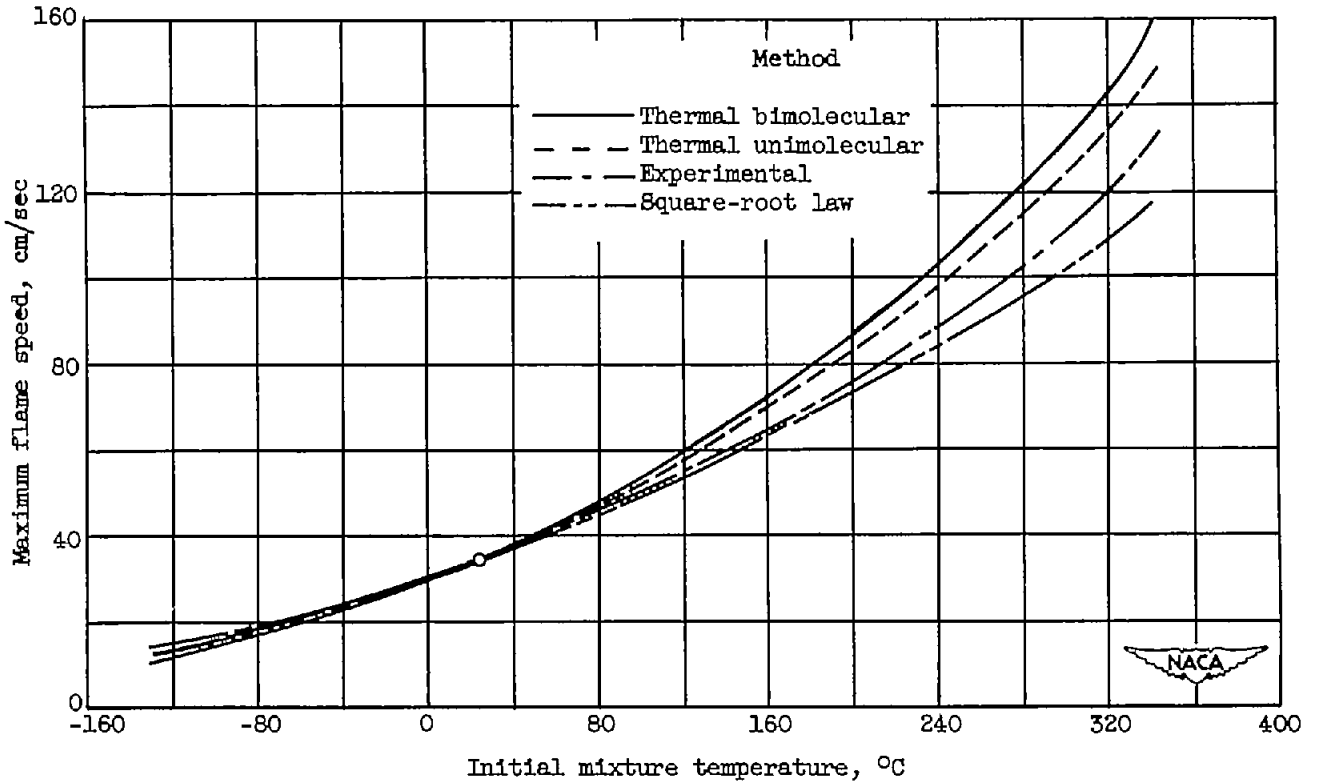

(a) Methane-air flames.

Figure 7. - Effect of initial mixture temperature on maximum flame speed. Comparison of theoretically predicted curves (based on 25° C) with experimental results.

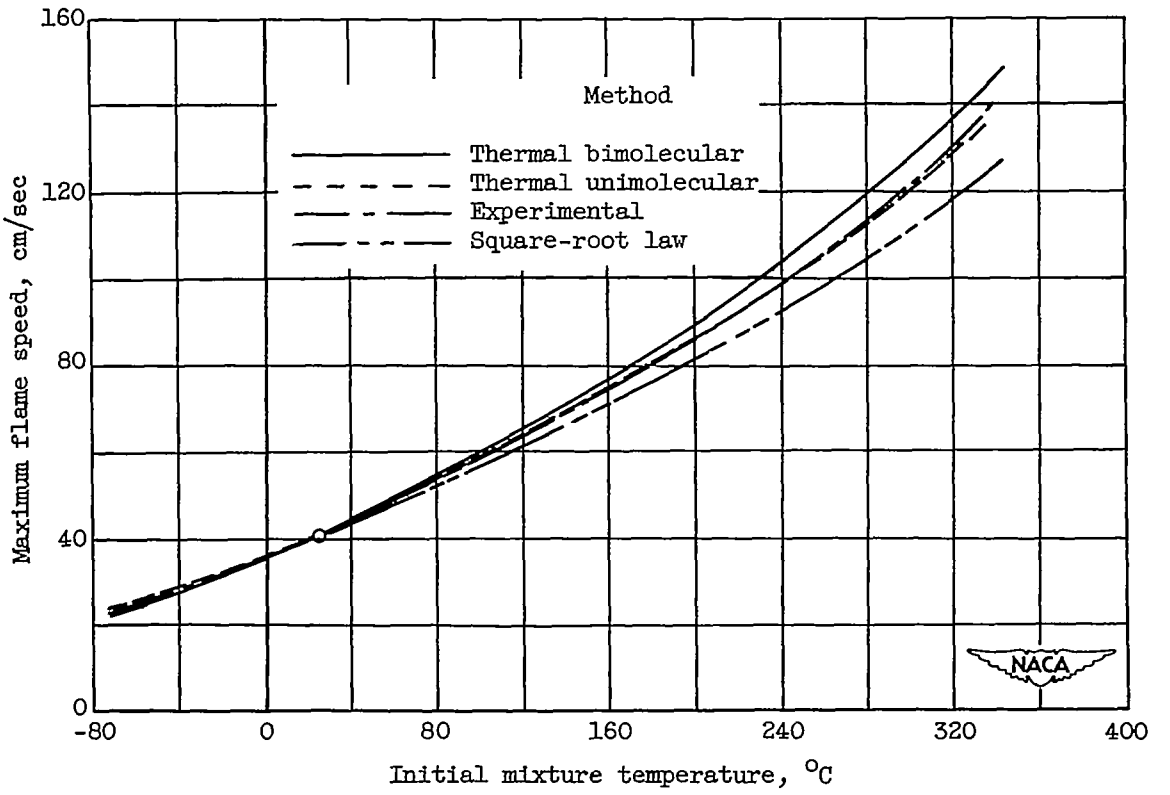

(b) Propane-air flames.

Figure 7. - Continued. Effect of initial mixture temperature on maximum flame speed. Comparison of theoretically predicted curves (based on 25° C) with experimental results.

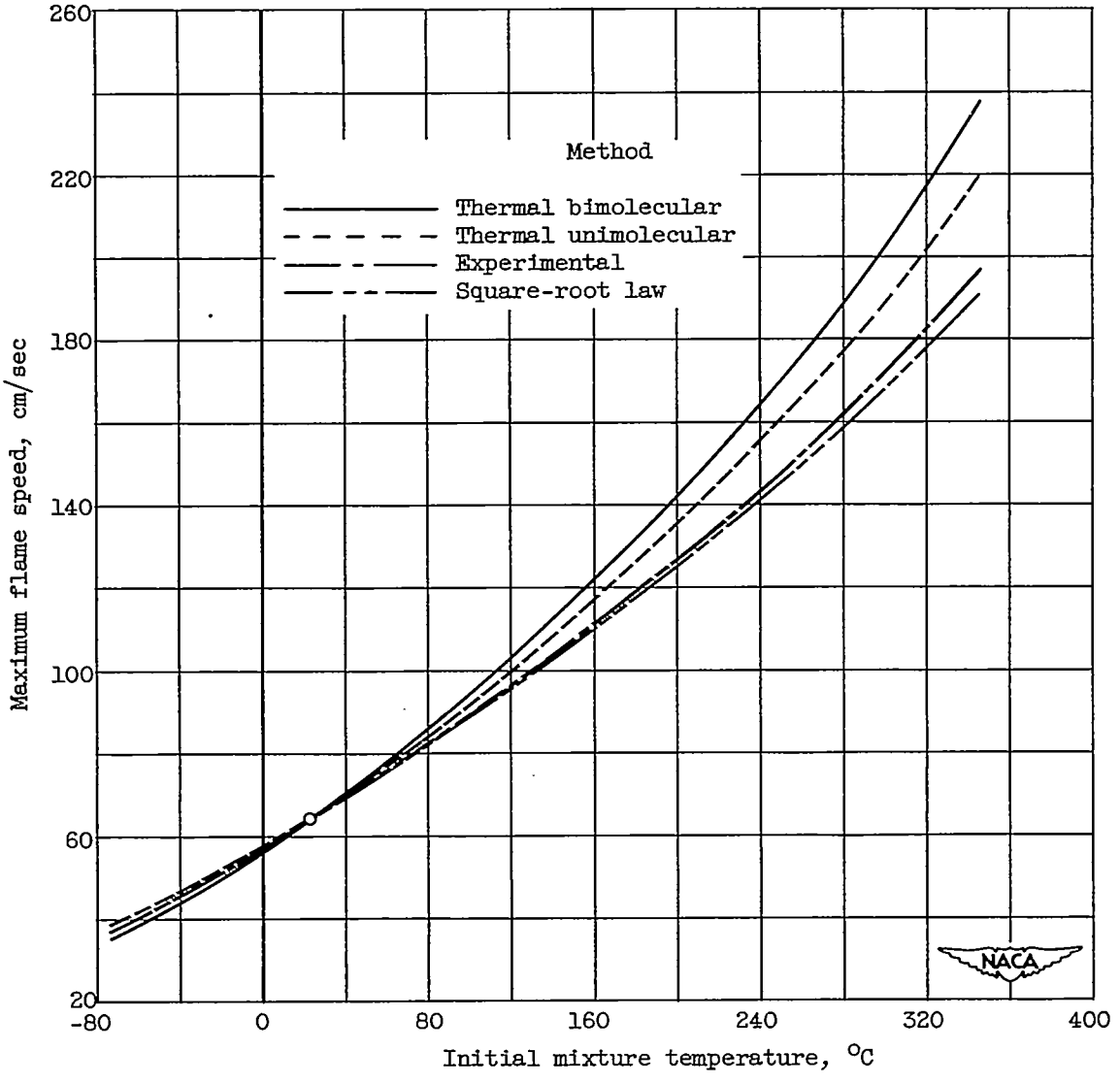

(c) Ethylene-air flames.

Figure 7. - Concluded. Effect of initial mixture temperature on maximum flame speed. Comparison of theoretically predicted curves (based on 25° C) with experimental results.

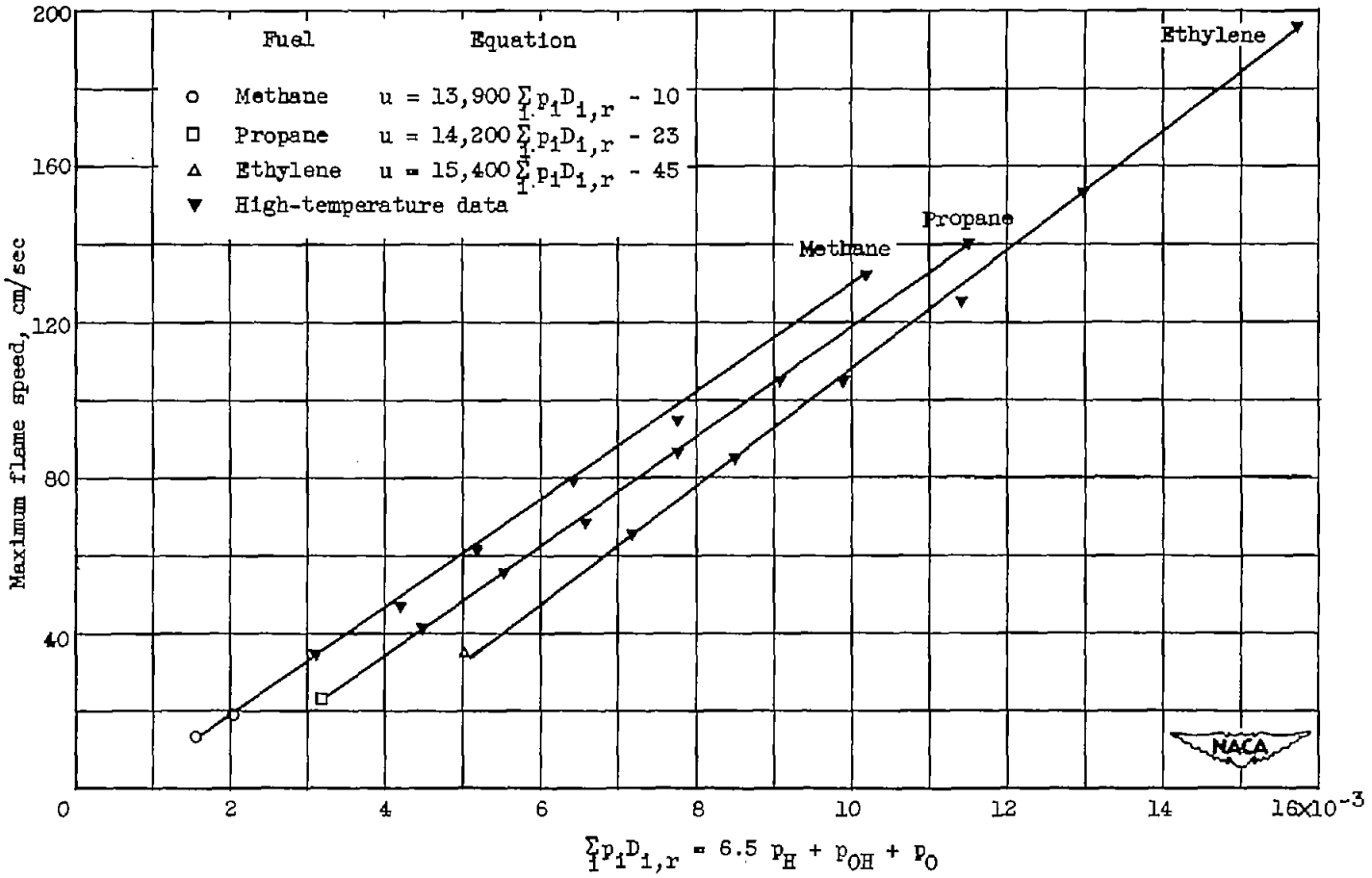

(a) Summation of effective-relative-radical pressures at flame temperatures based on sodium D-line measurements.

Figure 8. - Correlations between maximum flame speed and calculated equilibrium-radical concentrations.

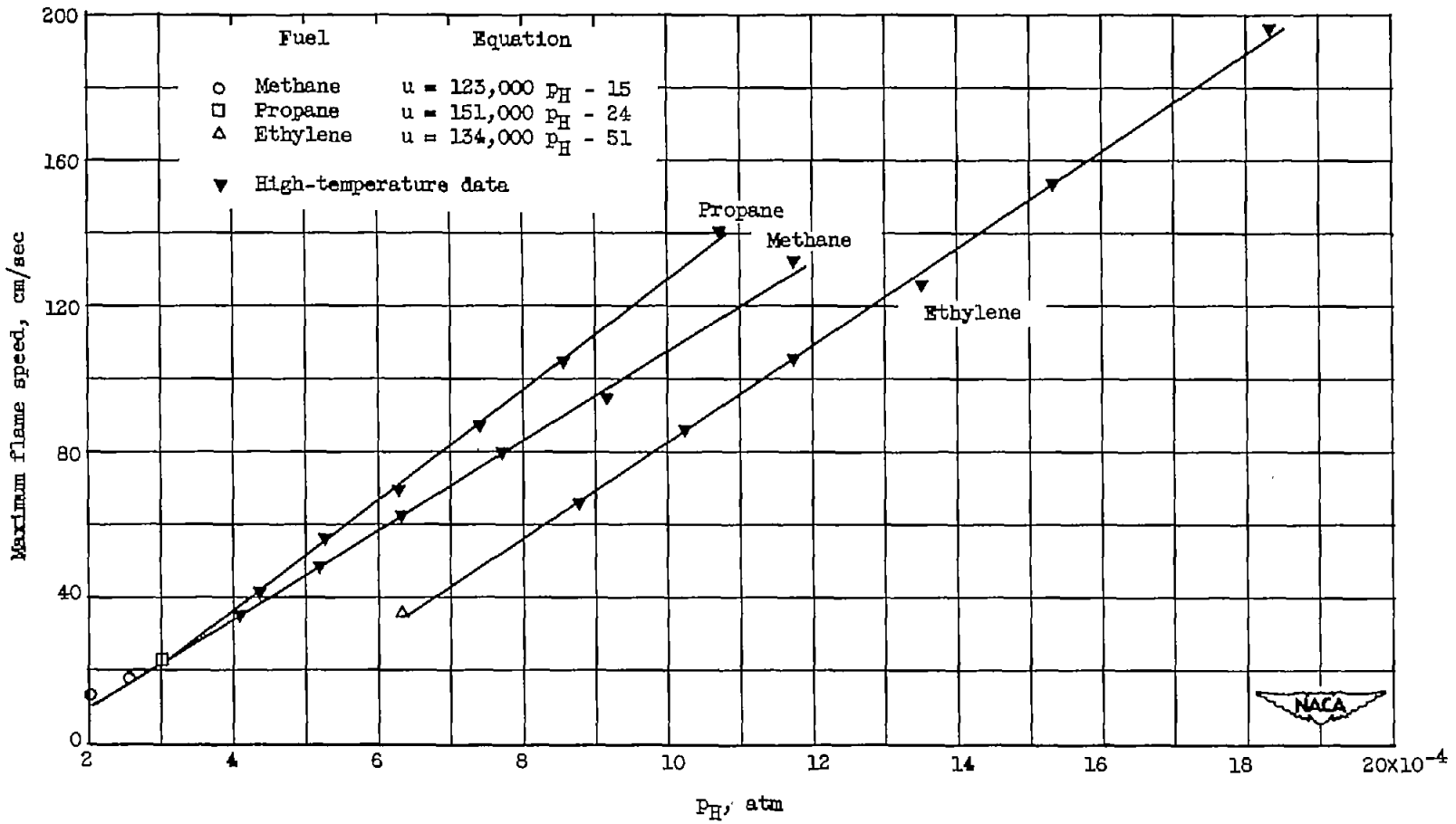

(b) Hydrogen-atom concentration at flame temperature based on sodium D-line measurement.

Figure 8. - Continued. Correlations between maximum flame speed and calculated equilibrium-radical concentrations.

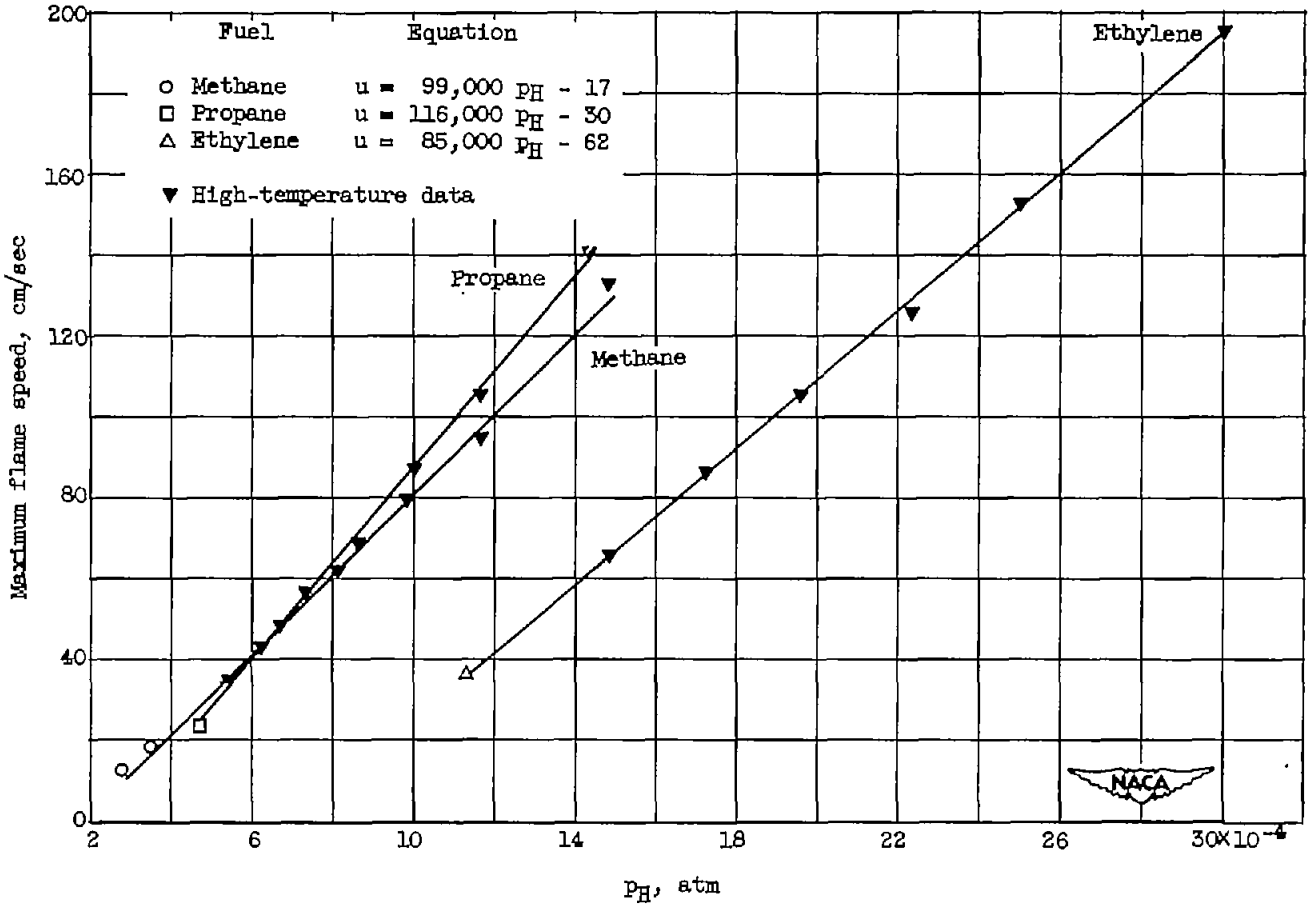

(c) Hydrogen-atom concentration at adiabatic flame temperature.

Figure 8. - Concluded. Correlations between maximum flame speed and calculated equilibrium-radical concentrations.